International Journal of Computer Science and Information Technology
ISSN: 3005-9682 (Print), ISSN: 3005-7140 (Online) | Volume 3, Number 3, Year 2024
DOI: https://doi.org/10.62051/ijcsit.v3n3.37
Journal homepage: https://wepub.org/index.php/IJCSIT/index

# Neural Network Adaptive Controller Design for Air-Ground Heterogeneous Formation

Shidong Chen *, Xianguo Tuo, Qinwen Deng, Qiang Han

School of Automation and Information Engineering, Sichuan University of Science & Engineering, Yi'bin, China

*Corresponding Author: Shidong Chen

## ABSTRACT

The air-ground heterogeneous multi-intelligent body formation cooperative control problem is addressed by proposing an adaptive controller heterogeneous multi-intelligent body formation cooperative control method based on radial basis function (RBF). The heterogeneous intelligent body formation, consisting mainly of unmanned ground vehicles (UGV) and unmanned aerial vehicles (UAV), is analyzed. Firstly, the equivalent transformations of the nonlinear dynamics models of UAVs and UGVs are derived, and a unified formation control model with acceleration as the control input is established. Secondly, the error model between the leader (UAV) and the follower (UGV) is established by adopting the leader-follower method. An adaptive controller with radial basis function (RBF) is designed to adjust the network weights online by sigmoid function and tanh function, ensuring that the tracking error of the formation converges to zero quickly. Finally, MATLAB simulations demonstrate that the joint formation of UAVs and unmanned vehicles can form the desired formation rapidly and achieve formation consistency.

## KEYWORDS

Heterogeneous formations; Leader-follower; Equivalent transformations

## 1. INTRODUCTION

In recent years, the rapid development of artificial intelligence and mobile robotics has brought increasing benefits. These advancements range from large-scale applications such as autonomous vehicles and medical service robots to smaller-scale devices like smartphones and smart wearables, all of which are closely related to human life. With technological progress and increased productivity, multi-robot cooperation has become a hot topic in the research field of multi-agent systems. Compared to single-agent systems, multi-agent cooperation has characteristics such as wide area coverage, strong environmental adaptability, and high task execution rates, attracting widespread interest from researchers in this field. In industrial scenarios, collaborative robots are being used in manufacturing, such as mobile robots in logistics warehouses for orderly delivery. Nevertheless, robot cooperation in civilian areas still faces significant challenges, such as the need to interact with humans and be deployed in unknown environments [1]-[3]. In civilian applications, search and rescue is a key scenario where the cooperation of heterogeneous robots can potentially save lives through faster response times [4][5]. In search and rescue operations, multi-robot cooperation can also significantly improve the efficiency of rescuers and speed up the search for victims. First, the search and rescue area is determined, and UAVs are used for preliminary exploration, real-time mapping of the environment, and real-time monitoring of rescue operations or establishing communication networks in emergencies. Finally, unmanned vehicles are used for path planning and material transportation.

Therefore, the UAV/UGV air-ground cooperative system can provide greater advantages for search and rescue and exploration missions.

Drones, especially multi-rotor UAVs, have become a research hotspot in the current robotics field due to their novel structural layout, unique flight methods, and relatively low cost. They can quickly navigate obstacles, rough terrain, or steep slopes and provide aerial views from high altitudes [6]. However, the payload and battery life of drones are limited, making it difficult for them to perform tasks requiring heavy equipment or complex operations.

Unmanned ground vehicles (UGVs) are a research hotspot in the current field of automatic control. On one hand, in road traffic, this technology has great potential to improve traffic safety, efficiency, comfort, and convenience. On the other hand, UGVs have higher battery capacity and larger payload, meaning they can carry heavier sensors, more powerful computers, and complex operational equipment to perform tasks [7]. However, they are often limited by sensor range, terrain traversal ability, and climbing capability.

In summary, forming heterogeneous joint formations of drones and unmanned vehicles provides more advantages than formations of either drones or unmanned vehicles alone in completing specific tasks, such as extensive area inspections, geographical surveys, armed searches, rescue, and transportation missions [8]. Some scholars have conducted research on the control issues of heterogeneous UAV/UGV joint formations and have achieved preliminary results.

The main control strategies for joint formations include behavior-based methods, virtual structure methods, and leader-follower methods. Reference [9] proposes a behavior-based formation control strategy for the formation and maintenance of joint formations. Reference [10] proposes a virtual structure-based control method for the landing problem of heterogeneous UAV and UGV systems. Reference [11] proposes a virtual structure-based controller to guide the formation for the collaborative task problem of heterogeneous unmanned systems. Reference [12] proposes an adaptive dynamic controller based on the virtual structure method for the payload problem of UAVs. Reference [13] studies time-varying formation tracking control, proposing continuous-time and discrete-time distributed formation tracking protocols through sliding mode control theory, with virtual experiments demonstrating the effectiveness of these protocols. Reference [14] designs a new distributed sliding mode control law for fixed-wing UAV formation control, where the control law for follower UAVs uses only their information and the leader's information, achieving the desired formation under constraints of linear and angular velocities. Reference [15] proposes an adaptive control method based on the leader-follower structure to address the problem of formation maintenance under wind field interference, effectively estimating the magnitude and direction of wind force in space to control the relative movement of UAVs and counteract the distance errors caused by wind field interference. Among these, the leader-follower control strategy has high control precision and is relatively easy to implement, providing a good approach for controlling heterogeneous UAV/UGV joint formations.

In controlling UAV/UGV air-ground joint formations, the differences in their dynamic models must be considered. The differences between the two models can lead to inconsistencies in control target quantities, increasing the difficulty of designing formation controllers. Additionally, to quickly form the desired formation, the controller for the air-ground joint formation needs to respond quickly. Reference [16] proposes a BP neural network control algorithm for distributed collaborative control of UAV formation systems. However, traditional BP neural networks have drawbacks such as slow convergence rates.

Based on the above analysis, this paper adopts the leader-follower control strategy to design a heterogeneous UAV/UGV air-ground joint formation structure, enhancing the stability and reliability of the joint formation. Equivalent transformations are used to process the two nonlinear dynamic models separately, extracting a common control target quantity—acceleration. To shorten the time required for rapid formation, an adaptive formation controller based on RBF neural networks is proposed, adjusting the weights online to accelerate convergence. This allows the heterogeneous UAV/UGV air-ground joint formation error to quickly approach zero and remain stable, while the joint formation can achieve formation consistency.

## 2. FORMATION MODELING

The heterogeneous UAV/UGV air-ground joint formation consists of three identical drones and three identical unmanned ground vehicles. According to the requirements of the predetermined formation and the states of adjacent unmanned vehicles and the leader, the drones and unmanned vehicles adjust their positions, speeds, and attitudes in real-time to meet the needs of joint formation control.

The main task of the UAV/UGV joint formation control is to achieve formation consistency. In this paper, a control strategy is proposed where the UAVs act as leaders and the UGVs as followers. An RBF neural network is used to design the formation controller. One UAV, serving as the leader, sends the desired position and speed information to the RBF neural network formation controller, while the remaining unmanned vehicles send their actual position and speed information to the controller. The formation controller adjusts the acceleration based on the direction of the position and speed error changes of the other unmanned vehicles, thereby adjusting their positions, speeds, and attitudes in real-time. This ensures that the unmanned vehicles quickly achieve formation maintenance. The structure of the heterogeneous UAV/UGV air-ground joint formation control system is shown in Figure 1.

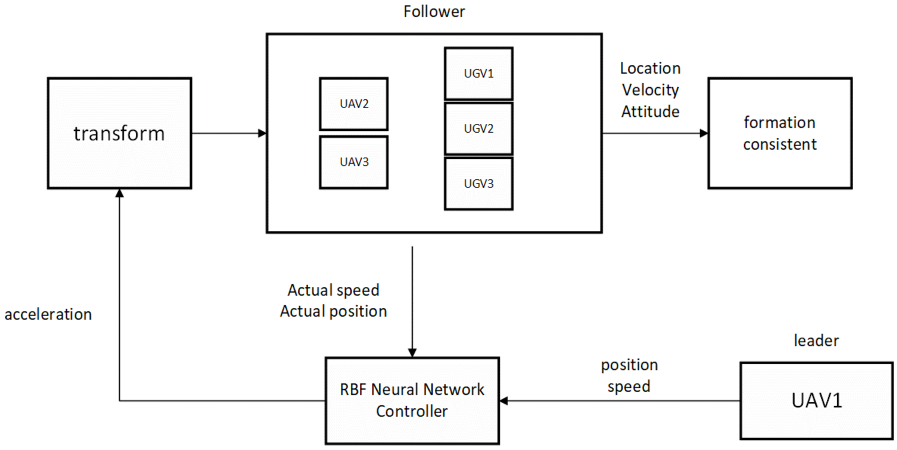


**Figure 1.** Structure of the Heterogeneous UAV/UGV Air-Ground Joint Formation Control System

Due to the differences in the models of UAVs and UGVs, the control target quantities are inconsistent. The following will separately explain the process of extracting the common control target quantity—acceleration—for the heterogeneous models.

$$\begin{cases} \dot{p}_{ax} = (\cos\phi_a \sin\theta_a \cos\psi_a + \sin\phi_a \sin\psi_a)\dfrac{F}{M_a} \\ \dot{p}_{ay} = (\cos\phi_a \sin\theta_a \sin\psi_a - \sin\phi_a \cos\psi_a)\dfrac{F}{M_a} \\ \dot{p}_{az} = \cos\phi_a \cos\theta_a \dfrac{F}{M_a} - g \end{cases} \tag{1}$$

Here, $m$ represents the mass, $g$ the gravitational acceleration, and $p_{ax}, p_{ay}, p_{az}$ the position of the UAV. $\phi_a, \theta_a, \psi_a$ represent the roll, pitch, and yaw angles, respectively. $F$ denotes the lift force of the UAV.

Using equivalent transformations to process Equation (1), we obtain:

$$\begin{cases} \phi_a = \arcsin(M_a \dfrac{\ddot{p}_{ax}{}^2 \sin\psi_a - \ddot{p}_{ay}{}^2 \cos\psi_a}{F}) \\ \theta_a = \arctan(\dfrac{\ddot{p}_{ax}{}^2 \cos\psi_a - \ddot{p}_{ay}{}^2 \sin\psi_a}{\ddot{p}_{ay}{}^2 + g}) \\ F = M_a \sqrt{\ddot{p}_{ax}{}^2 + \ddot{p}_{ay}{}^2 + (\ddot{p}_{az}{}^2 + g)^2} \end{cases} \tag{2}$$

A two-wheeled differential drive wheeled mobile robot is selected as the UGV, and its nonlinear dynamic model is as follows:

$$\begin{cases} \dot{p}_{gx} = v\cos\psi_g \\ \dot{p}_{gy} = v\sin\psi_g \end{cases} \tag{3}$$

Here, $\psi_g = \omega, \dot{v} = F / M_g, \dot{\omega} = \varepsilon / J_g$, $\dot{p}_{gx}, \dot{p}_{gy}$ represents the speed of the UGV, $v, \omega$ denote the linear and angular velocities of the UGV, $\psi_g$ represents the yaw angle of the UGV, $M_g, J_g$ denote the mass and moment of inertia of the UGV, $\varepsilon$ represents the input torque, and $F$ represents the resultant force acting on the UGV.

Using equivalent transformations to process Equation (3), we obtain:

$$\begin{bmatrix} \ddot{p}_{gx}^h \\ \ddot{p}_{gy}^h \end{bmatrix} = \begin{bmatrix} \cos\psi_g & \text{-}\sin\psi_g \\ \sin\psi_g & \cos\psi_g \end{bmatrix} \begin{bmatrix} F - l_g \omega^2 \\ \tau l_g / J_g + V\omega \end{bmatrix} \tag{4}$$

Here, $\ddot{p}_{gx}, \ddot{p}_{gy}$ represents the acceleration of the UGV, and $l_g$ represents the length of the UGV.

After applying equivalent transformations to the UAV and UGV models, it is evident that the attitude, lift, and acceleration of the UAV are interrelated, while the resultant force and torque of the UGV are also related to its acceleration. Thus, a unified control model with acceleration as the control input can be established for the joint formation:

$$u = [\ddot{p}_{xh} \ \ddot{p}_{yh} \ \ddot{p}_{zh}]^T \tag{5}$$

# 3. DESIGN OF THE FORMATION CONTROLLER BASED ON RBF NEURAL NETWORK

When the state variables of the unmanned vehicles change rapidly, the leader-follower strategy can ensure the stability and reliability of the formation. At the same time, the RBF network joint formation controller can quickly respond to formation requirements.

## 3.1. Leader-Follower Formation Structure

The Unmanned Aerial Vehicle (UAV) is selected as the leader and the Unmanned Ground Vehicle (UGV) is selected as the follower, and the set of relative positions and velocities of the leader (UAV) with respect to with respect to the follower (UGV) is, and the set of relative positions and velocities of the follower (UGV) with respect to the leader (UAV) is $F_{ij}$.

$$\begin{cases} L_{ij} = \left\{ p_{aij}^x, p_{aij}^y, p_{aij}^z, v_{aij}^x, v_{aij}^y, v_{aij}^z \right\} i, j = 1, 2, 3\cdots \\ F_{ij} = \left\{ p_{ij}^x, p_{ij}^y, p_{ij}^z, v_{ij}^x, v_{ij}^y, v_{ij}^z \right\} i, j = 1, 2, 3\cdots \end{cases} \tag{6}$$

A heterogeneous formation is composed of three UAVs and three UGVs. The network topology of the leader-follower formation strategy is shown in Figure 2.

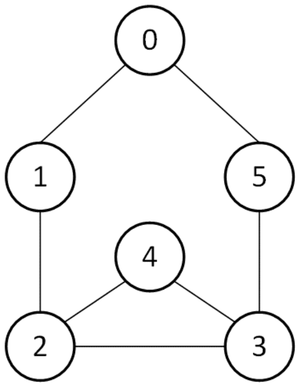

**Figure 2.** Communication Topology of the Leader-Follower Air-Ground Heterogeneous System

When $\lim_{t\to\infty} L_{ij} = L_{ij}{}^{d}, \lim_{t\to\infty} F_{ij} = F_{ij}{}^{d}$, it indicates that the desired formation has been achieved. Here, $L_{ij}{}^{d}, F_{ij}{}^{d}$ represents the desired state matrix. Further derivation yields:

$$\begin{cases} P_i^d = \delta(p_f^d - p_l) + \sum_{j\in N_i}^{\infty} \chi(p_{ij}^d - p_j) \\ V_i^d = \delta(v_f^d - v_l) + \sum_{j\in N_i}^{\infty} \chi(v_{ij}^d - v_j) \end{cases} \tag{7}$$

Here, $p_l, v_l$ represent the position and velocity of the leader, while $p_f^d, v_f^d$ represent the desired position and velocity of the follower. $p_{ij}, v_{ij}$ denote the position and velocity between adjacent unmanned vehicles, and $\delta, \chi$ represents the weight.

It can be seen that the error model established between the leader unmanned vehicle and the follower unmanned vehicles using the leader-follower strategy can enhance the stability and reliability of the heterogeneous air-ground joint formation of unmanned vehicles.

### 3.2. RBF Neural Network Formation Controller

To ensure a rapid response for the air-ground heterogeneous formation controller, an RBF neural network is used to design the formation controller. The joint formation error model is: $e(x) = (p_d - p, v_d - v)$, When the air-ground heterogeneous formation is stable: $\lim_{x\to\infty} |e(x)| = 0$.

In the RBF network, the traditional Gaussian function has a slower convergence rate, while the reflective sigmoid function converges faster, significantly reducing the convergence time for the joint formation. The function is expressed as follows:

$$h_j = 1/(1+\exp(\frac{\|x-c_j\|^2}{2b_j^2})) \tag{8}$$

Here, $x$ represents the network input, and $j$ represents the $j$ network input in the hidden layer.

Under the leader-follower control strategy, the input of the RBF network is $x = [e_p \ e_v \ p_d \ v_d]^T$, where $e_p, e_v$ represents the position error and velocity error of the unmanned vehicle, and $p_d, v_d$ represents the desired position and desired velocity of the unmanned vehicle.

Define the error function as $E = e_v + \zeta e_p$, and $\zeta > 0$.

$f(x)$ is the neural network approximation function. The design of the air-ground heterogeneous joint formation control law :

$$g(x) = f(x) + \varepsilon_f + \varepsilon_g \tag{9}$$

Where $g(x) = u(x)$ is the control input for formation control, $\varepsilon_f, \varepsilon_g$ is the network approximation error.

The learning algorithm for RBF network weights, base parameters, and center vectors:

$$\begin{cases} A_n(s) = A_n(s\text{-}1) + \Delta A_n(s)(\alpha + 1) \\ B_n(s) = B_n(s-1) + \eta \Delta B_n(s) + \alpha(B_n(s-1) - B_n(s-2)) \\ C_{in}(s) = C_{in}(s-1) + \eta \Delta C_{in}(k) + \alpha(C_{in}(s-1) - C_{in}(s-2)) \end{cases} \tag{10}$$

Where $\eta$ is the learning rate, and $\alpha$ is the momentum factor.

From equation（10）, it is clear that the size of the learning rate $\eta$ affects the adjustment of weights, thereby influencing the convergence speed of the algorithm. When $\eta$ is too small, the convergence speed is slow. When $\eta$ is too large, weight adjustments are large, which may cause oscillations near the minimum during the convergence process. Simple weight adjustments do not significantly improve the convergence speed of the joint formation network. Therefore, further adaptive adjustments to $\eta$ and $\alpha$ are necessary to enhance the training speed of the RBF network by adaptively adjusting the learning rate.

The definitions are as follows:

$$e(s) = \frac{|E(s)| - |E(s-1)|}{E(s)} \tag{11}$$

$$L(s) = \begin{cases} L(s-1)(1 + e^{\varsigma e(s)}), e(s) < 0 \\ L(s-1)(1 - e^{\varsigma e(s)}), e(s) > 0 \end{cases} \tag{12}$$

$$\eta(s) = \begin{cases} m_1 \eta(s-1), E(s-1) > E(s) \\ m_2 \eta(s-1), E(s-1) < E(s) \\ \eta(s-1), E(s-1) = E(s) \end{cases} \tag{13}$$

$$\alpha(k) = \sigma t \tanh(L(s) \frac{\partial E}{\partial A(s)}) \tag{14}$$

Where $L(s)$ is the parameter required for the $k$ learning iteration, $\varsigma, \sigma$ are constants, $m_1 > 1$, and $0 < m_2 < 1$

From the above analysis, it is evident that the improved weight adjustment algorithm adjusts the learning rate and momentum factor in response to error changes at each step. The function tanh can easily change the direction of weight adjustments, adaptively adjusting the learning rate and momentum factor in this algorithm, thereby accelerating the learning rate, reducing steady-state error, decreasing convergence time, and ultimately rapidly reducing tracking errors to zero while maintaining stability.

## 4. SIMULATION ANALYSIS AND RESULTS

Simulation involves 3 UAVs and 3 UGVs to validate the proposed leader-follower control strategy (7) and RBF network algorithm (9) in the heterogeneous air-ground joint formation. The initial states are shown in Tables 1 and Tables 2:

**Table 1.** Initial State of UGV

| UGV(1) | UGV(2) | UGV(3) |
|---|---|---|
| Position(10,0)m | Position(15,0)m | Position(0,15)m |
| Speed(10,0)m/s | Speed(15,5)m/s | Speed(10,5)m/s |

**Table 2.** Initial State of UAV

| UAV(1) | UAV(2) | UAV(3) |
|---|---|---|
| Position(5,10,10)m | Position(10,5,5)m | Position(10,10,10)m |
| Speed(0,10,0)m/s | Speed(0,10,0)m/s | Speed(0,10,0)m/s |
| Attitude(0,0,0)°<br>Angle(0,0,0)° | Attitude(0,5,0)°<br>Angle(2,1,1)° | Attitude(0,0,5)°<br>Angle(1,2,1)° |

The basic parameters of the UAVs and UGVs are shown in Tables 3 and Tables 4.

**Table 3.** Basic Parameters of UGV

| name | m/kg | L/m | $j/kg{\cdot}m^2$ |
|---|---|---|---|
| value | 21 | 0.5 | 1 |

**Table 4.** Basic Parameters of UAV

| name | m/kg | L/m | $I_X/kg{\cdot}m^2$ | $I_Y/kg{\cdot}m^2$ | $I_Z/kg{\cdot}m^2$ |
|---|---|---|---|---|---|
| value | 1.93 | 0.21 | 0.15 | 0.15 | 0.18 |

The simulation time is 50 seconds, with a step size of 0.02 seconds. Figure 3 shows the attitude, velocity, position, and error curves of the joint formation. In Figure 3(a), the yaw angle of the formation stabilizes at 12 seconds, and the formation moves in the predetermined direction. The roll angle of the UAV converges quickly, stabilizing at around 10 seconds, while the pitch angle converges more slowly, stabilizing at around 12 seconds, mainly because the UAV needs to gain forward speed during forward motion. Figure 3(b) indicates that the formation's speed stabilizes at around 20 seconds. Figure 3(c) shows the planar position curve of the heterogeneous formation, demonstrating that the heterogeneous air-ground joint formation quickly achieves the desired formation, with fast position convergence. In summary, the leader-follower control strategy (7) and the RBF network algorithm (9) for the heterogeneous air-ground joint formation are rapid and effective.

Figure 4 shows the comparison of position error curves between the traditional RBF and the improved RBF. Under the traditional RBF network, the position error fluctuates periodically, making it difficult to achieve stability. The improved RBF reduces the error stabilization time by 8% and lowers the steady-state error by 7.5%. It features smaller overshoot, faster convergence, shorter adjustment time, and smaller steady-state error, resulting in a smoother transition. This validates that the improved RBF network (13) (14) has better control performance.

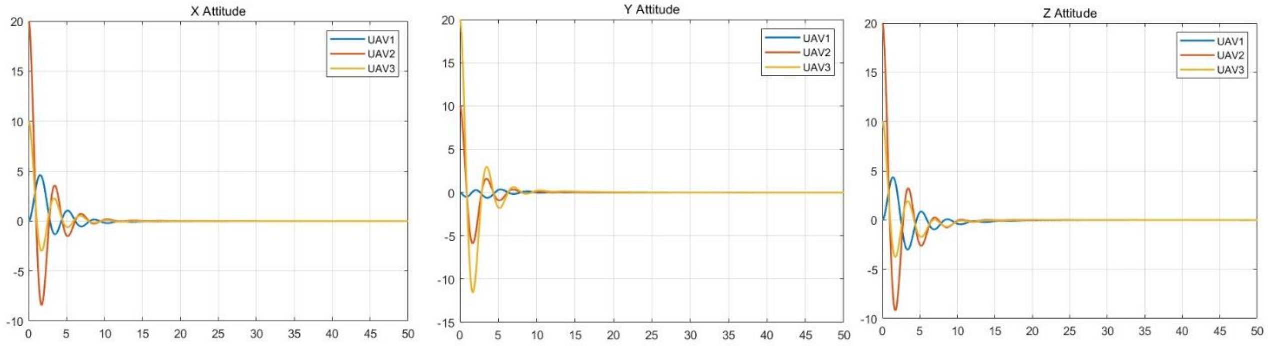


(a) Attitude

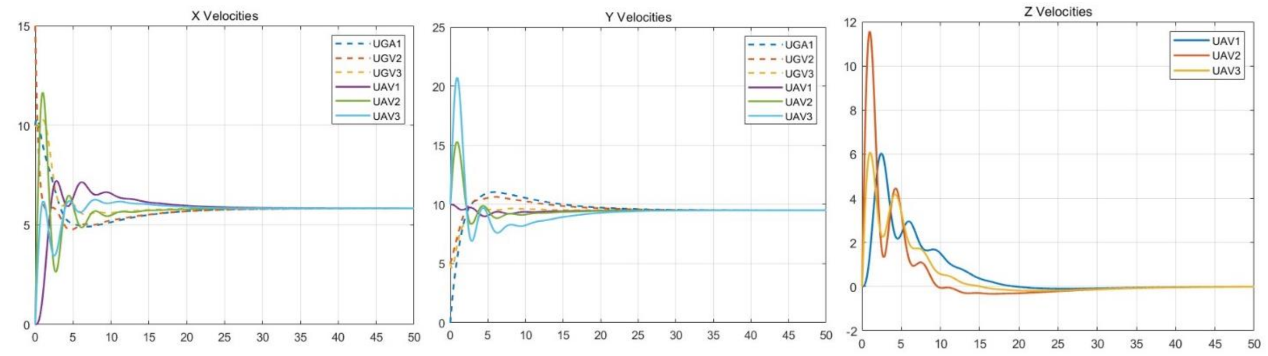


(b) speed

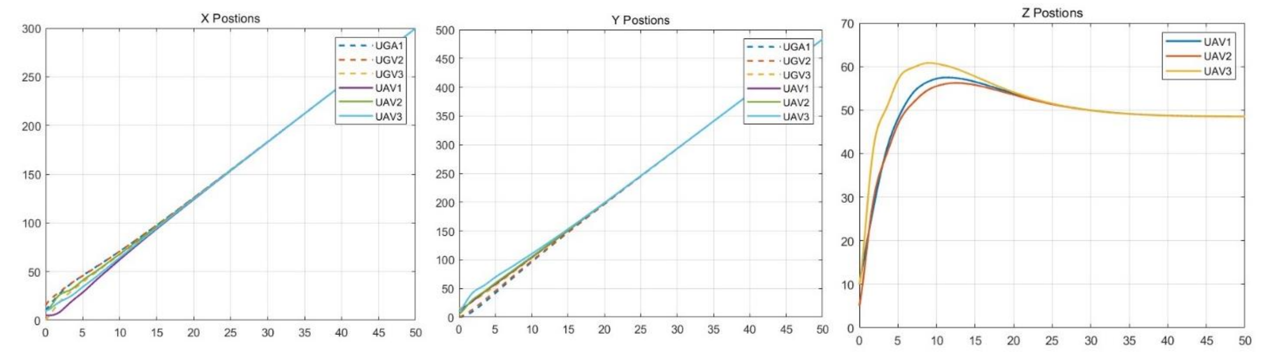


(c) position

**Figure 3.** Attitude, Velocity, and Position of Heterogeneous Formation

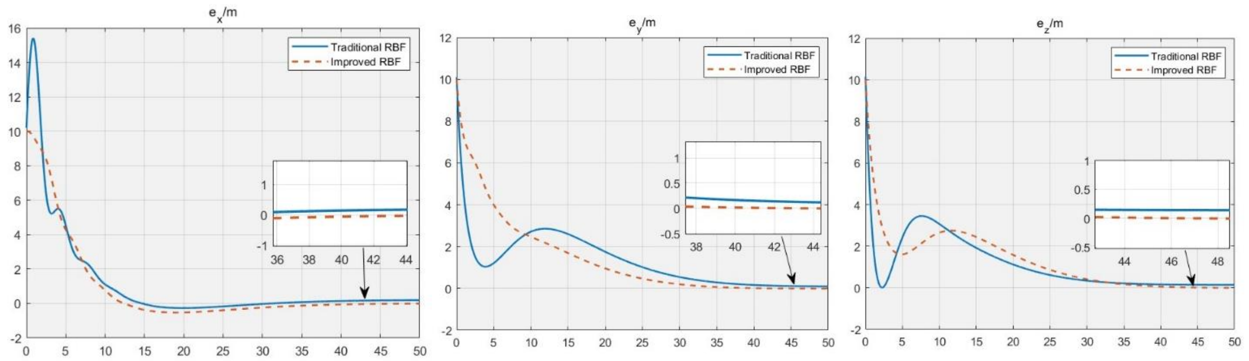


(a) X-direction error (b) Y-direction error (c) Z-direction error

**Figure 4.** Comparison of Errors between Traditional RBF and Improved RBF

# 5. CONCLUDE

This paper combines the leader-follower control strategy with RBF networks to design a heterogeneous air-ground joint formation control algorithm that exhibits strong stability and fast tracking capabilities. Simulation results demonstrate that the designed controller effectively achieves the desired formation, and the improved weight adjustment method adapts to error models, enhancing formation stability and reliability. By utilizing sigmoid and tanh functions to enhance the learning rate of the controller, the stabilization time of errors has been reduced by 8%, and the steady-state error of the system has decreased by 7.5%. This algorithm provides valuable insights for the application of heterogeneous UAV-Ground Vehicle formations.

# REFERENCES


[1] Ingrand F, Ghallab M. Deliberation for autonomous robots: A survey [J]. Artificial Intelligence, 2017, 247: 10-44.

[2] Deng C, Liu G, Qu F, et al. Survey of important issues in multi unmanned aerial vehicles imaging system [J]. Int. J. Softw. Hardware Res. Eng, 2018:12:28-38.

[3] Shakhatreh H, Sawalmeh A H, Al-Fuqaha A, et al. Unmanned aerial vehicles (UAVs): A survey on civil applications and key research challenges [J]. Ieee Access, 2019, 7: 48572-48634.

[4] Mehmood S, Ahmed S, Kristensen A S, et al. Multi criteria decision analysis (mcda) of unmanned aerial vehicles (uavs) as a part of standard response to emergencies[C]//4th International Conference on Green Computing and Engineering Technologies. Gyancity International Publishers, 2018, 31:77-92.

[5] Middletona W T, Millera G, Pollmana A. Cooperative Unmanned, Air-Ground Vehicle Search and Rescue Exercise [J]. 2018,54:186-203

[6] Tmušić G, Manfreda S, Aasen H, et al. Current practices in UAS-based environmental monitoring [J]. Remote Sensing, 2020, 12(6): 1001-1019.

[7] Hayat S, Yanmaz E, Muzaffar R. Survey on unmanned aerial vehicle networks for civil applications: A communications viewpoint [J]. IEEE Communications Surveys & Tutorials, 2016, 18(4): 2624-2661.

[8] Kuo R J, Lee Y H, Zulvia F E, et al. Solving bi-level linear programming problem through hybrid of immune genetic algorithm and particle swarm optimization algorithm [J]. Applied Mathematics and Computation, 2015, 266: 1013-1026.

[9] Liu W, Zheng X, Deng Z. Adaptive distributed formation maintenance for multiple UAVs: exploiting proximity behavior observations [J]. Journal of Central South University, 2021, 28(3): 784-795.

[10] Wang Y, Cheng Z.control based on multi–agent system consensus [J]. IEEE Access, 2020, 8: 49000-49012.

[11] Bacheti V P, Brandão A S, Sarcinelli-Filho M. Path-following with a ugv-uav formation considering that the uav lands on the ugv[C]//2020 International Conference on Unmanned Aircraft Systems (ICUAS). IEEE, 2020,8:488-497.

[12] Villa D K D, Brandao A S, Carelli R, et al. Cooperative load transportation with two quadrotors using adaptive control [J]. IEEE Access, 2021, 9: 129148-129160.

[13] Wang J, Han L, Dong X, et al. Distributed sliding mode control for time-varying formation tracking of multi-UAV system with a dynamic leader [J]. Aerospace Science and Technology, 2021, 111: 106549.

[14] Wang X, Yu Y, Li Z. Distributed sliding mode control for leader-follower formation flight of fixed-wing unmanned aerial vehicles subject to velocity constraints [J]. International Journal of Robust and Nonlinear Control, 2021, 31(6): 2110-2125.

[15] Zhang J, Zhang P, Yan J. Distributed adaptive finite-time compensation control for UAV swarm with uncertain disturbances [J]. IEEE Transactions on Circuits and Systems I: Regular Papers, 2020, 68(2): 829-841.

[16] Xiang T, Liao X, Wong K. An improved particle swarm optimization algorithm combined with piecewise linear chaotic map [J]. Applied Mathematics and Computation, 2007, 190(2): 1637-1645.